

Etch Characteristics of Magnetic Tunnel Junction Materials Using Bias Pulsing in the CH₄/N₂O Inductively Coupled Plasma

Min Hwan Jeon¹, Ji Youn Youn¹, Kyung Chae Yang², Deok Hyun Yun², Du Yeong Lee³,
Tae Hun Shim³, Jea Gun Park³, and Geun Young Yeom^{1,2,*}

¹SKKU Advanced Institute of Nano Technology (SAINT), Sungkyunkwan University,
Suwon, Gyeonggi-do 440-746, South Korea

²Department of Materials Science and Engineering, Sungkyunkwan University,
Suwon, Gyeonggi-do 440-746, South Korea

³Department of Electronics Engineering, Hanyang University, Seoul 133-791, South Korea

The etch characteristics of magnetic tunneling junction (MTJ) related materials such as CoFeB, MgO, FePt, Ru, and W as hard mask have been investigated as functions of rf pulse biasing, substrate heating, and CH₄/N₂O gas combination in an inductively coupled plasma system. When CH₄/N₂O gas ratio was varied, at CH₄/N₂O gas ratio of 2:1, not only the highest etch rates but also the highest etch selectivity over W could be obtained. By increasing the substrate temperature, the linear increase of both the etch rates of MTJ materials and the etch selectivity over W could be obtained. The use of the rf pulse biasing improved the etch selectivity of the MTJ materials over hard mask such as W further. The surface roughness and residual thickness remaining on the etched surface of the CoFeB were also decreased by using rf pulse biasing and with the decrease of rf duty percentage. The improvement of etch characteristics by substrate heating and rf pulse biasing was possibly related to the formation of more stable and volatile etch compounds and the removal of chemically reacted compounds more easily on the etched CoFeB surface. Highly selective etching of MTJ materials over the hard mask could be obtained by using the rf pulse biasing of 30% of duty ratio and by increasing the substrate temperature to 200 °C in the CH₄/N₂O (2:1) plasmas.

Keywords: RF Pulsed ICP, Selective Etching, Magnetic Tunnel Junction Materials, Substrate Heating, CH₄/N₂O Gas Mixture.

1. INTRODUCTION

Recently, a variety of nonvolatile memory devices have been paid great attention due to the limited memory performance of existing memory devices.^{1,2} Among them, spin transfer torque magnetic random access memory (STT-MRAM) device is one of the promising semiconductor memory devices owing to high density storage, high speed, infinite rewrite, low power consumption, etc.³⁻⁷

In the case of STT-MRAM device, the magnetic tunnel junction (MTJ) stack which is composed of ferromagnetic layer/dielectric tunneling barrier layer/ferromagnetic layer is the most important because the main data are recorded in the MTJ stack.^{8,9} For the mass storage, high speed and non-volatile STT-RAM devices, the highly selective

etching of multi-layered MTJ stack needs to be developed. However, MTJ-related materials do not easily form the volatile compounds at low substrate temperatures and, for conventional halogen-based etch gases, corrosion of etched MTJ stack tends to occur during the etching.¹⁰⁻¹² Therefore, these materials have been etched by physical sputtering rather than conventional reactive ion etching methods. For the etching of MTJ materials, etch residue is formed on the sidewall of the etched MTJ stack due to the low volatility and it leads to a leakage current path during the operation of MRAM devices. Also, the leakage current is increased by physical damage of the sidewall of the MTJ stack by the ion bombardment with high energy ions during sputtering. To overcome the etch problems, several research groups have been investigated the etching of magnetic materials using non-corrosive gas

* Author to whom correspondence should be addressed.

mixtures to increase the formation of volatile compounds between etchant gas such as CH₄/Ar, CO/NH₃, CH₃OH, etc.^{13–18} However, these reactive gases do not easily form the stable and volatile carbonyl compounds and tend to show very low etch rates due to difficulty in reacting with MTJ materials using conventional plasma etching methods.

Previously, to increase the formation of volatile and stable metal carbonyl compounds between MTJ materials and etch gas, a pulse-biased inductively coupled plasma (ICP) technique has been investigated for CO/NH₃ by applying 13.56 MHz pulsed rf power to the substrate while the ICP source power is continuously applied to the plasma.¹⁹ By using the pulse-biased ICP technique, the etch selectivity of MTJ materials over W could be improved with decreasing the pulse duty ratio. Also, the surface roughness and residual thickness of the etched CoFeB surface were gradually decreased with the decrease of pulse duty ratio possibly due to the formation of the more volatile and more stable etch compounds during the pulse-off time. The increase of substrate temperature can also increase the etch rates and etch selectivities of MTJ materials over mask materials. A previous study on the etching of MTJ materials by the substrate heating to 120 °C with CH₃OH gas in a conventional ICP system showed the increase of etch rates of MTJ materials at the elevated substrate temperature even though they concluded that the increase of MTJ etch rate is more responsible for the formation of pure metal at the elevated temperature than by the formation of volatile and stable etch compounds.¹⁸

In this study, the effect of rf pulse-biasing and substrate heating on the etching of MTJ materials using an ICP system have been studied with a CH₄/N₂O gas mixture (after the optimization of the optimum CH₄:N₂O ratio). The etch characteristics have been investigated to increase the etch rates and etch selectivities of MTJ materials over mask materials further and to investigate the possibility of forming volatile and more stable etch compounds.

2. EXPERIMENTAL DETAILS

The MTJ-related materials such as CoFeB, FePt, Ru, and MgO and a hard mask material such as W were prepared to investigate the etch characteristics in an inductively coupled plasma (ICP) system. The ICP etch system used in this experiment is an eight-inch diameter commercial etcher (STS PLC, UK) and the schematic diagram of the ICP system used in this study is shown in Figure 1. As shown in this figure, one-turn inductive coil was wound around the ceramic chamber wall and a 13.56 MHz rf power was connected to the inductive coil. Also, a separate 13.56 MHz rf power was applied to the substrate for rf pulse biasing, and the substrate was heated from room temperature (RT) up to 200 °C using an oil heater (P5, LAUDA). The 13.56 MHz pulsed rf power was applied to the substrate using a pulse/function generator (8116A,

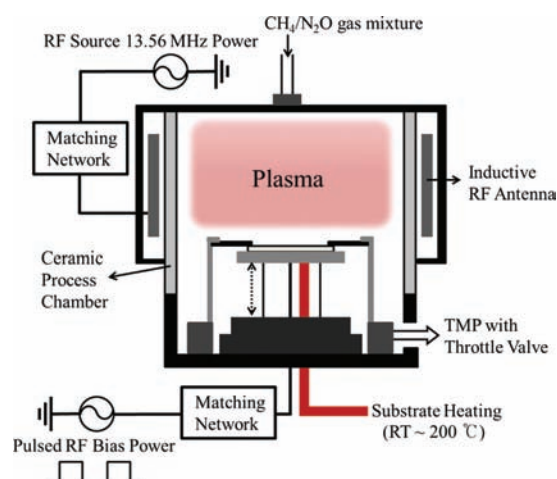


Figure 1. Schematic diagram of the pulse-biased ICP etching system used in this study.

HP), a signal generator (8657B, HP), and an rf power amplifier (A1000, ENI).

Blank MTJ-related materials such as CoFeB, FePt, MgO, Ru, and blank W were used to investigate the etch characteristics such as etch rate and etch selectivity. These materials were etched using CH₄/N₂O gas combination with various gas ratios. The ICP source power of 500 W and DC bias voltage of -300 V (time-averaged DC bias voltage) to the substrate were used to etch the MTJ-related materials. During the rf pulse biasing, time-averaged DC biasing was used to compensate the decrease of etch rates by the pulsing. (that is, for example, to maintain the time-averaged DC bias voltage of -300 V for $x\%$ duty ratio, the instant DC bias voltage of $-300 \times (100/x\%)$ V was applied to the substrate during the pulse-on time.) The process pressure and the total flow rate were fixed at 5 mTorr and 50 sccm, respectively.

After the etching of the MTJ-related materials, a step profilometer (Alpha step 500, Tencor) was used to measure the etch depth. To investigate the chemical bonding characteristics of the residue remaining on the CoFeB surface, etched CoFeB samples were investigated using X-ray photoelectron spectroscopy (XPS, ESCA2000, VG Microtech Inc.) using a Mg $K\alpha$ twin-anode source. The surface morphology of CoFeB after the etching was analyzed with a high resolution atomic force microscope (HR AFM, SPA-300HV).

3. RESULTS AND DISCUSSION

Using CH₄/N₂O gas combination, the effect of gas ratio on the etch characteristics of MTJ-related materials such as CoFeB, FePt, MgO, Ru, W and their etch selectivities over W were investigated and the results are shown in Figure 2(a) for the etch rates and (b) for the etch selectivities. The rf power to the ICP source was 13.56 MHz CW 500 W and the DC bias voltage to the substrate was -300 V by applying a separate 13.56 MHz CW rf power.

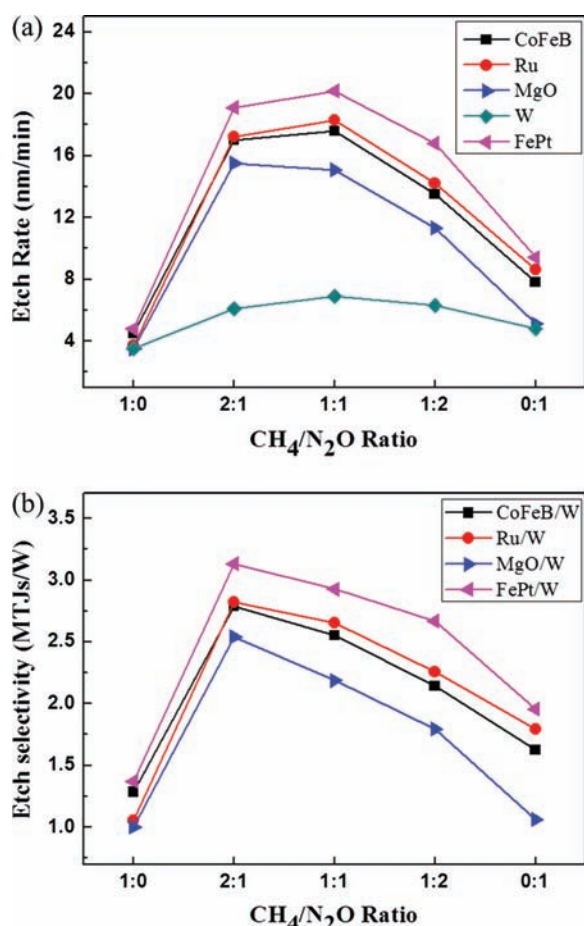


Figure 2. Etch rates of MTJ materials and W and etch selectivities of MTJ materials over W as a function of $\text{CH}_4/\text{N}_2\text{O}$ gas combination at RT. (a) etch rates of MTJ materials and (b) etch selectivities of MTJ materials over W as a function of $\text{CH}_4/\text{N}_2\text{O}$ gas ratio.

The operating pressure was maintained at 5 mTorr while flowing 50 sccm of $\text{CH}_4/\text{N}_2\text{O}$ total gas flow rate. The substrate temperature was kept at RT. As shown in Figure 2(a), the etch rates were increased with the increase of N_2O ratio in the $\text{CH}_4/\text{N}_2\text{O}$ gas mixture and showed the maximum at the ratio of $\text{CH}_4:\text{N}_2\text{O} = 1:1$ for CoFeB, Ru, FePt, and W and at the ratio of $\text{CH}_4:\text{N}_2\text{O} = 1:1$ for MgO, and the further increase of N_2O ratio in the gas mixture decreased the etch rates. The highest etch rates for FePt, Ru, and CoFeB were 20.2, 18.3, and 17.6 nm/min, respectively. The highest etch rates obtained at the gas mixture of $\text{CH}_4:\text{N}_2\text{O} = 1\sim 2:1$ appear to be related to the formation of volatile compounds between the MTJ-related materials and reactive gas combination the most easily at this gas composition. The etch selectivities of MTJ-related materials over W also showed the maximum at the ratio of $\text{CH}_4:\text{N}_2\text{O} = 2:1$ and the highest etch selectivities of CoFeB, Ru, MgO, and FePt over W were 2.78, 2.82, 2.54, and 3.13.

To investigate the chemical reactivity between the MTJ-related materials and the etch gas mixture and the possible volatility of the etch products, the effect of substrate

temperature on the etch rates and etch selectivities was investigated at the $\text{CH}_4/\text{N}_2\text{O}$ gas ratio of 2:1 and the results are shown in Figure 3. The other etch conditions are kept the same as those in Figure 2. As shown in Figure 3(a), the increase of the substrate temperature from RT to 200 °C increased the etch rates of all of the materials investigated. The increased etch rates of MTJ-related materials with increasing the substrate temperature are believed to be related to the increased chemical reactivity between MTJ-related materials and the $\text{CH}_4/\text{N}_2\text{O}$ gas mixture and the increased volatility of the etch compounds formed by the reactions. By increasing the substrate temperature to 200 °C, the etch rates of CoFeB, Ru, MgO, and FePt were increased to 23.4, 24.8, 21.1, and 25.9 nm/min. Possibly due to the less reactivity of W with the etch gas mixture, the increase of W etch rate with increasing substrate temperature was the lowest. Therefore, as shown in Figure 3(b), the etch selectivities of CoFeB, Ru, MgO, and FePt over W were increased with the increase of substrate temperature and showed the highest values of 3.3, 3.5, 3.0, and 3.0,

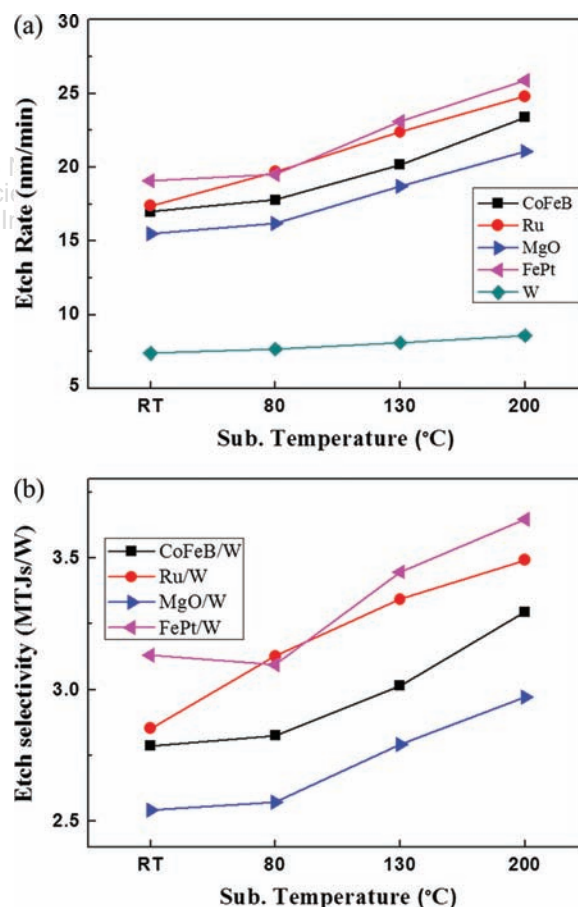


Figure 3. Etch rates of MTJ materials and W and etch selectivities of MTJ materials over W as a function of substrate temperature at the $\text{CH}_4/\text{N}_2\text{O}$ gas combination of 2:1. (a) etch rates of MTJ materials and (b) etch selectivities of MTJ materials over W as a function of substrate temperature.

and 3.7 at 200 °C, respectively, in addition to the highest etch rates.

The improved etch selectivities obtained in Figure 3 by increasing the substrate temperature to 200° may not be enough for the etching of MTJ materials. To increase the reactivity of MTJ-related materials with CH₄/N₂O further, the substrate was rf pulse biased instead of rf CW biasing and the effect of pulse duty ratio on the etch rates and etch selectivities of MTJ-related materials was investigated. Figures 4(a) and (b) show the effect of the rf pulse duty ratio on (a) the etch rates and (b) the etch selectivities of MTJ-related materials investigated. The substrate temperature was maintained at 200 °C and the CH₄/N₂O gas ratio was maintained at 2:1 at the total gas flow rate of 50 sccm. The operating pressure was maintained at 5 mTorr and 500 W of 13.56 MHz CW rf power was applied to the ICP source. The substrate was 13.56 MHz rf pulse biased at different duty ratios from 100 (CW) to 30% while keeping the time averaged DC bias voltage at -300 V and the pulse frequency at 50 kHz. The use of rf pulse biasing generally decreases the etch rates due to the

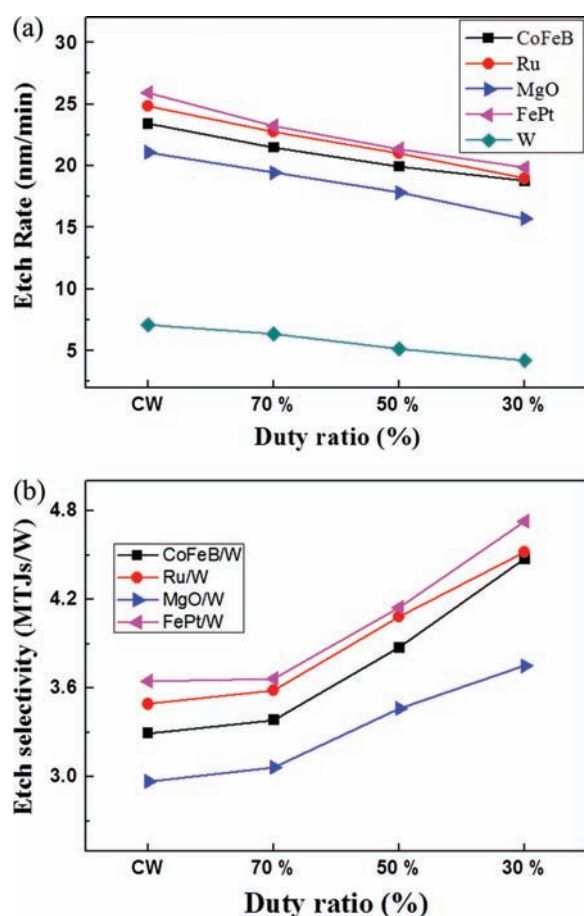


Figure 4. Etch rates of MTJ materials and W and etch selectivities of MTJ materials over W as a function of rf pulse duty ratio of the substrate biasing for the CH₄/N₂O gas combination of 2:1 and at 200 °C of substrate temperature. (a) etch rates of MTJ materials and (b) etch selectivities of MTJ materials over W as a function of pulse duty percentage.

Table I. Vapor pressure, melting point, or boiling point of MTJ materials.

	Vapour pressure or melting and boiling point	References
Co	Co ₂ (CO) ₈ : 3.2 × 10 ⁻³ kPa at 288 °K log P(kPa) = 12.79 - 4420/T	[20]
Fe	Fe(CO) ₅ : 1.97 kPa at 288 °K log P(mmHg) = 8.45 - 2096.7/T	[20, 21]
B	B ₂ H ₆ melting point: 108.15 °K B ₂ H ₆ boiling point: 180.4 °K	[22]
Pt	Pt(CO) ₄ melting point: 298 °K	[23]
Ru	Ru(CO) ₅ melting point: 251 °K	[24]
W	W(CO) ₆ : 9.7 × 10 ⁻⁴ kPa at 288 °K log P(kPa) = 10.66 - 3886/T	[20]

pulse-off time where no etching is occurred due to lack of ion bombardment, therefore, to compensate the significant decrease of etch rates with decreasing the pulse duty ratio, the time averaged DC pulse bias voltage condition (for example, for 50% duty ratio, -600 V of DC bias voltage was used during the pulse-on time for the substrate biasing to have time averaged DC bias voltage of -300 V) was used. As a result, as shown in Figure 4(a), the etch rates of MTJ-related materials were decreased only slightly with the decrease of rf pulse duty percentage by using the time averaged DC bias condition of -300 V. On the other hand, the etch selectivities were increased continuously with decreasing the duty ratio. The increased etch selectivity with decreasing the rf duty ratio is believed to be related to the formation of more volatile etch compound during the pulse-off time without breaking the stable etch product molecules such as metal carbonyls by the ion bombardment and the increased removal of etch products by high energy ion bombardment during the pulse-on time. Table I shows the possible volatile metal carbonyls formed with MTJ materials by the reaction with CH₄/N₂O during the pulse-off time. As shown in Table I, possibly due to the higher vapor pressures of Co(CO)₈ and Fe(CO)₅ compared to W(CO)₆, the etch selectivity appeared to be increased by forming those stable metal carbonyl molecules during the longer pulse-off time and at the increased substrate temperature. In addition, as shown in Table I, Pt and Ru also tend to form volatile metal carbonyls such as Pt(CO)₄, Ru(CO)₅, respectively.

The variation of surface roughness of MTJ-related materials with rf pulse biasing was investigated using AFM for CoFeB with the etch conditions shown in Figure 4 and the results are shown in Figure 5. The etch time was 3 minutes. As a reference, the surface roughness of the CoFeB before the etching was also measured and the result is included in the figure (pristine). Before the etching, the root-mean square (rms) surface roughness of CoFeB was 0.81 nm and, when the CoFeB was etched by the CW rf biasing, the rms surface roughness was increased to 4.83 nm possibly due to non-uniform etching of the CoFeB surface. However, as the rf duty ratio is decreased, the rms surface roughness was decreased and, when the duty ratio is

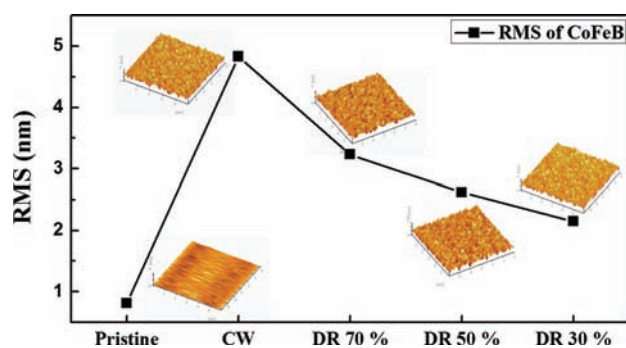


Figure 5. AFM surface roughness of the CoFeB etched as a function of rf pulse duty percentage. As a reference, the surface roughness of pristine CoFeB was also measured and the result is included in the figure. The etch time was 3 minutes.

30%, the rms surface roughness was decreased to 2.15 nm. The decrease of the rms surface roughness with decreasing the duty ratio is believed to be related to the formation of more uniform and more stable volatile etch compounds on the surface during the longer pulse-off time and the removal of those compounds more easily and more non-selectively due to the higher ion bombardment energy during the shorter pulse-off time as investigated in a previous study.²⁰

The differences in the chemical binding states of MTJ-related materials for the etching at CW biasing/RT (representing lower chemical reaction between MTJ materials and etch gas mixture and lower vaporization of the chemically reacted layer) and those at rf pulsing (30% duty ratio)/200 °C (representing higher chemical reaction and

higher vaporization of the chemically reacted layer) were measured using XPS. The other etch conditions are the same as those in Figure 5. Figure 6 shows XPS narrow scan data of Co 2*p*, Fe 2*p*, and B 1*s* for CoFeB etched at the conditions of the CW biasing/RT and the pulse biasing (30% duty ratio)/200 °C. The XPS data were taken every 90 sec during the depth profiling using an Ar⁺ ion gun (3 kV ion energy and 2 μA ion current) until 360 sec. In the case of pristine CoFeB, the binding energies were observed at 778.3 and 793.2 eV for Co 2*p*, 707 and 720.2 eV for Fe 2*p*, and 188 eV for B 1*s*. After the etching, for both etched at the conditions of the CW biasing/RT and the rf pulsing (30% duty ratio)/200 °C, additional higher binding energy peaks at 781 and 797.1 eV for Co 2*p*, 710 and 723.5 eV for Fe 2*p*, and 192 eV for B 1*s* were observed. These high binding energy peaks appear to be related to Co—O, Fe—O, and B—O bonding (or possibly also, Co—CO, Fe—CO, and B—CO) remaining on the CoFeB surface as the residue during the etching using $\text{CH}_4/\text{N}_2\text{O}$ similar to other etch gas combinations such as CO/NH_3 as investigated earlier.²⁰ Even though those additional peaks were observed similarly for both etch conditions, the peaks were removed earlier for the CoFeB etched at the rf pulsing (30% duty ratio)/200 °C during the XPS depth profiling indicating a thinner residue layer compared to the CoFeB etched at the condition of the CW biasing/RT possibly due to the increased chemical reaction on the surface and the increased volatility of etch products. The relative atomic percentages of the residue on the CoFeB surface etched with the conditions in Figure 6 were measured as a function of XPS depth profiling time and the

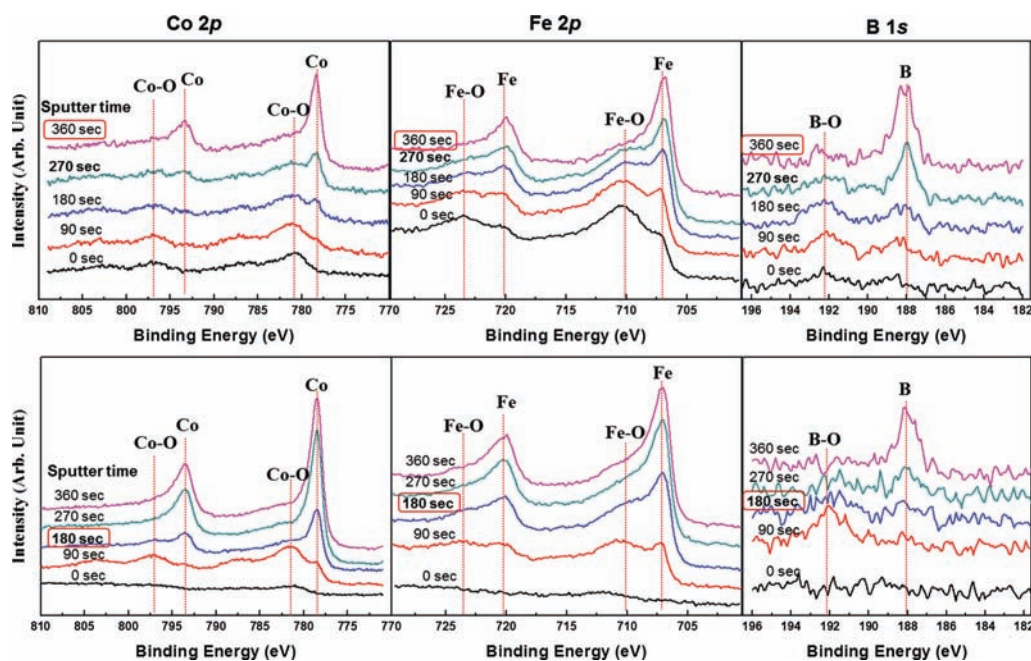


Figure 6. XPS narrow scan data of (a) Co 2*p*, (b) Fe 2*p*, and (c) B 1*s* during the depth profiling of the etched CoFeB surface for the etching condition of the rf CW biasing/RT and for the condition of the rf pulse biasing (30% duty)/200 °C. The CoFeB sample was etched using $\text{CH}_4/\text{N}_2\text{O}$ gas mixture for 3 minutes.

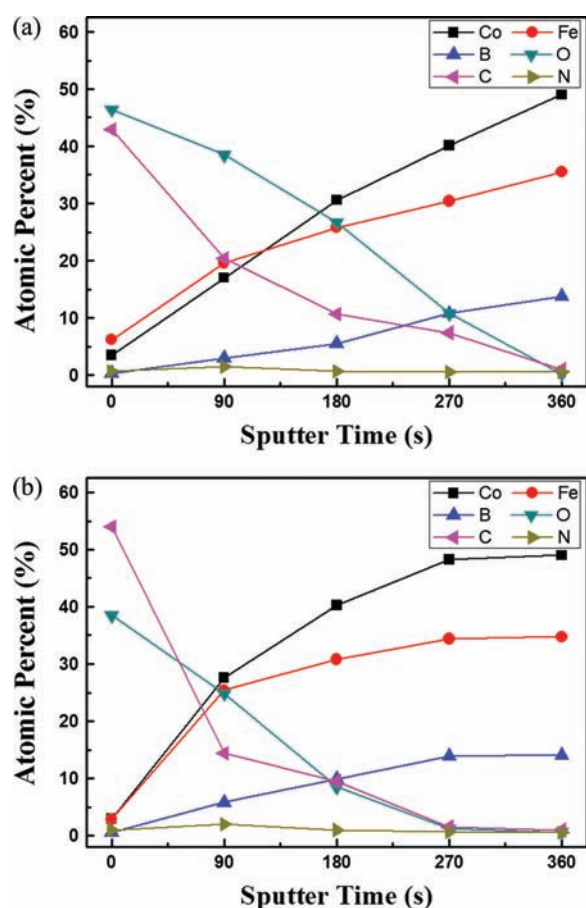


Figure 7. Relative atomic percentages of the etched CoFeB measured during XPS depth profiling as a function of Ar⁺ ion depth profiling time for the etching condition of the CW biasing/RT and for the condition of the pulse biasing (30% duty)/200 °C in Figure 6.

results are shown in Figure 7. The relative atomic percentage of CoFeB before the etching (pristine) was Co:Fe:B = 50.5%:36.5%:13%. As shown in the figures, after the etching using CH₄/N₂O, the surface of the etched CoFeB was carbon and oxygen-rich in addition to small Co, Fe, and B for both etch conditions of the CW biasing/RT and the pulse biasing (30% duty ratio)/200 °C possibly due to the dissociated carbon and oxygen from CH₄/N₂O etch gas. With the increase of depth profiling time, the carbon and oxygen percentages were decreased and the percentages of Co, Fe, and B were increased for both condition. However, as shown in the figure, the thickness of residue layer remaining on the CoFeB etched with the condition of CW biasing/RT was thicker than that etched with the condition of the pulse biasing (30% duty ratio)/200 °C by recovering the pure CoFeB surface after 360 sec and 180 sec of depth profiling time, respectively. The decrease of the residue layer remaining on the CoFeB etched with the heated and pulse biased condition is believed to be related to the increased stable etch compound formation and easier removal of the etch compound by the higher substrate temperature and by pulse biasing the substrate.

4. CONCLUSIONS

The etch characteristics of MTJ materials such as CoFeB, FePt, MgO, Ru and hard mask material such as W were investigated in a pulse-biased ICP system as functions of pulse duty ratio, CH₄/N₂O gas ratio, and substrate temperatures. When CH₄/N₂O gas combination was varied, the highest etch selectivity over W was obtained at CH₄/N₂O gas ratio of 2:1 and it is believed to be related to the highly chemical reaction between MTJ-related materials and reactive gases. By using the rf bias pulsing and by increasing the substrate temperature, the etch selectivity of MTJ materials such as CoFeB, FePt, MgO, Ru over W were improved further possibly due to the formation of more stable and volatile etch compounds and by the removal of chemically reacted compounds more easily on the etched CoFeB surface. In the etching of CoFeB, with the decrease of pulse duty ratio, the surface roughness and the thickness of etch residue were decreased and it is believed to be related to the formation of chemical reaction uniformly on the CoFeB surface during the pulse-off time and the non-selective removal of etch compounds during the pulse-on time. As a result, similar to other gas mixtures such as CO/NH₃ investigated earlier, more selective etching of MTJ materials over W could be observed by using the pulse biasing to 30% duty ratio and by increasing the substrate temperature up to 200 °C while etching using a CH₄/N₂O gas composition of (2:1) and the time-averaged DC bias voltage condition. At this condition, the residue thickness remaining on the etched CoFeB surface and the surface roughness were also the lowest.

Acknowledgments: This work was supported by the SRC project No. 2011-IN-2219. The authors would like to thank Dr. Satyarth Suri and Dr. Bob Turkot in Intel Corp. for helpful discussion on MRAM etching.

References and Notes

1. S. Tehrani, B. Engel, J. M. Slaughter, E. Chen, M. DeHerrera, M. Durlum, P. Naji, R. Whig, J. Janesky, and J. Calder, *IEEE Transactions on Magnetics* 36, 2752 (2000).
2. W. Reohr, H. Hoernigschmid, R. Robertazzi, D. Gogl, F. Pesavenot, S. Lammers, K. Lewis, C. Arndt, Y. Lu, H. Viehmann, R. Scheuerlein, L. K. Wwang, P. Trouilloud, S. Parkin, W. Gallagher, and G. Mueller, *IEEE Circuits and Devices* 18, 17 (2002).
3. M. C. Gaidis, E. J. O'Sullivan, J. J. Nowak, Y. Lu, S. Kanakasabapathy, P. L. Trouilloud, D. C. Worledge, S. Assefa, K. R. Milkove, G. P. Wright, and W. J. Gallagher, *IBM J. Res. and Dev.* 50, 41 (2006).
4. K. Lee and S. H. Kang, *IEEE Trans. Magn.* 46, 1537 (2010).
5. M. Pakala, Y. Huai, T. Valet, Y. Ding, and Z. Diao, *J. Appl. Phys.* 98, 056107 (2005).
6. K. Yakushiji, K. Noma, T. Saruya, H. Kubota, A. Fukushima, T. Nagahama, S. Yuasa, and K. Ando, *Appl. Phys. Express* 3, 053003 (2010).
7. A. Brataas, A. D. Kent, and H. Ohno, *Nat. Mater.* 11, 372 (2012).
8. J.-G. Zhu and C. Park, *Materials Today* 9, 36 (2006).
9. C. S. Ricardo and P. I. Lucian, *C. R. Physique* 6, 1013 (2005).
10. K. Ichihara and M. Hara, *Jpn. J. Appl. Phys.* 36, 4874 (1997).

11. K. B. Jung, E. S. Lambers, J. R. Childress, S. J. Pearton, M. Jenson, and A. T. Hurst, *Appl. Phys. Lett.* 71, 1255 (1997).
12. C. G. C. H. M. Fabrie, J. T. Kohlhepp, H. J. M. Swagten, B. Koopmans, M. S. P. Andriess, and E. vander Drift, *J. Vac. Sci. Technol. B* 24, 2627 (2006).
13. X. Peng, S. Wakeham, A. Morrone, A. Axdal, M. Feldbaum, J. Hwu, T. Boonstra, Y. Chen, and J. Ding, *Vacuum* 83, 1007 (2009).
14. N. Matsui, K. Mashimo, A. Egami, A. Konishi, O. Okada, and T. Tsukada, *Vacuum* 66, 479 (2002).
15. H. Kubota, K. Ueda, Y. Ando, and T. Miyazaki, *J. Magn. Magn. Mater.* 272–276, E1421 (2004).
16. X. Kong, D. Krasa, H. P. Zhou, W. Williams, S. McVitie, J. M. R. Weaver, and C. D. W. Wilkinson, *Microelectron. Eng.* 85, 988 (2008).
17. K. Kinoshita, T. Yamamoto, H. Honjo, N. Kasai, S. Ikeda, and H. Ohno, *Jpn. J. Appl. Phys.* 51, 08HA01 (2012).
18. M. S. Lee and W. L. Lee, *Appl. Surf. Sci.* 258, 8100 (2012).
19. M. H. Jeon, H. J. Kim, K. C. Yang, S.-K. Kang, K. N. Kim, and G. Y. Yeom, *Jpn. J. Appl. Phys.* 52, 05EB03 (2013).
20. M. L. Garner, D. Chandra, and K. H. Lau, *J. Phase Equilibria* 16, 24 (1995).
21. A. G. Gilbert and K. G. P. Sulzmann, *J. Electrochem. Soc.* 121, 832 (1974).
22. D. R. Lide, *Handbook of Chemistry and Physics*, 84th edn., CRC Press, Boca Raton, FL (2004), pp. 5–7.
23. http://www.webelements.com/compounds/platinum/platinum_tetracarbonyl.html.
24. C. W. Bradford, *Platinum Metals Rev.* 16, 50 (1972).

Received: 10 July 2013. Accepted: 12 February 2014.

IP: 127.0.0.1 On: Thu, 25 Nov 2021 14:54:28
Copyright: American Scientific Publishers
Delivered by Ingenta